Predicting the location of avulsion hazards on deltas in the face of changing flood regimes

Austin J. Chadwick & Michael P. Lamb
Division of Geological and Planetary Sciences, California Institute of Technology

RESNICK INSTITUTE
science + energy + sustainability

1. Motivation

On densely populated deltas, the tendency for river channels to catastrophically avulse poses a hazard to human life and property.

Previous work has shown that river avulsions preferentially occur around a location that is set by backwater hydrodynamics, the interplay of dynamic river discharge and standing water near the shoreline.

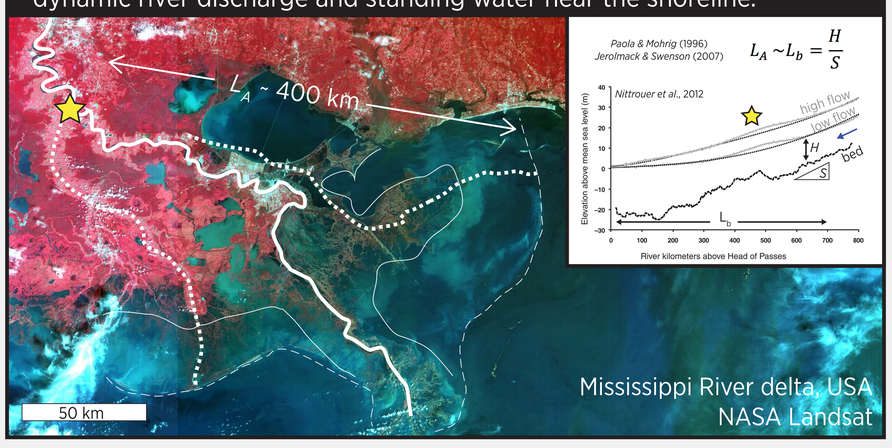

Our ability to forecast the location of future avulsion events is limited because avulsions are relatively rare and many deltas are experiencing drastic changes in flood regime due to land-use and climate change.

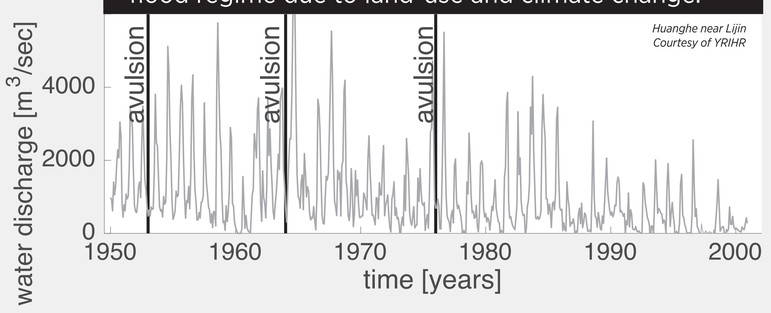

Research question: How do differences in flood regime affect the location of river avulsions on deltas?

2. Conceptual model

Quasi-2D Flow hydraulics and sediment mass-balance govern the long-profile evolution of a sinuous channel & delta lobe complex.

$$\frac{dH}{dx} = \frac{S - S_f}{1 - Fr^2} + \frac{Fr^2}{1 - Fr^2}\frac{H}{B}\frac{dB}{dx}$$ backwater equation
(Chow, 1959; Parket et al., 2008a; Chatanantavet et al., 2012; Lamb et al., 2012)

$$C_f q_t = \sqrt{RgD^3}\alpha(\tau^*)^n$$ sediment transport relation
(Engelund & Hansen, 1967)

$$\frac{\partial \eta_b}{\partial t} + \sigma = -\frac{(1+\Lambda)\Omega}{(1-\lambda_p)B_f}\frac{\partial B q_t}{\partial x}$$ Exner equation
(Parker et al., 2004; Chatanantavet et al., 2012)

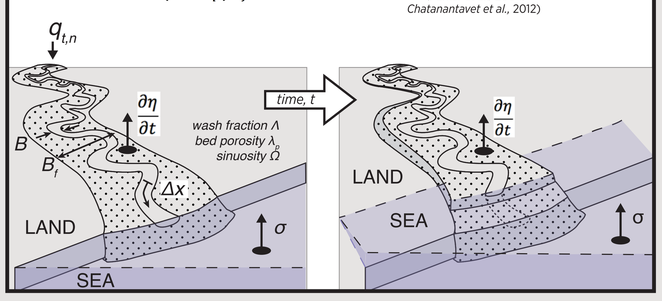

Avulsions are set up through superelevation of delta lobes relative to one another.

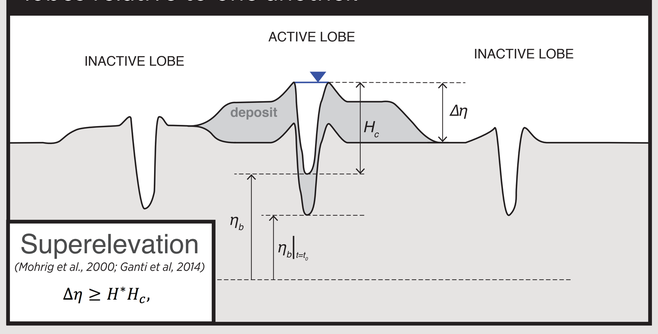

At times of avulsion, flow reoccupies old channels that pave the shortest available path to the shoreline.

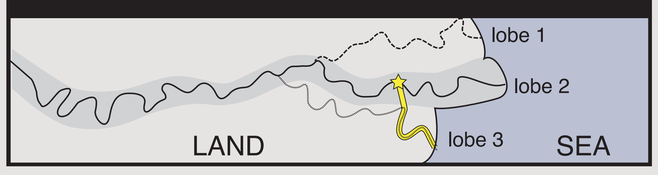

We perform a dimensional analysis using upstream reach dimensions and mean sediment supply.

$$\eta = \eta^* H_0, \qquad x = x^* L_b, \qquad B = B^* B_0,$$

$$t = t^* T_{adj} = t^* \frac{H_0 B_f L_b}{B \bar{q}_t} \frac{(1-\lambda_p)}{\Omega(1+\Lambda)},$$

$$\frac{\partial H^*}{\partial x^*} = \frac{S^* - S_f^*}{1 - Fr^2} + \frac{Fr^2}{1 - Fr^2}\frac{H^*}{B^*}\frac{dB^*}{dx^*}$$

$$C_f q_t^* = \alpha(\tau^*)^n,$$

$$\frac{\partial \eta^*}{\partial t^*} + \sigma^* = -\frac{1}{\bar{q}^*_t}\frac{\partial B^* q_t^*}{\partial x^*},$$

$H_n^*(t^*) = \frac{H_n(t)}{H_{n,bf}}$ ← model input

$L_A^* = \frac{L_A}{L_b} = x_s^* - x^*|_{\Delta\eta^* \geq H^*}$ ← model output

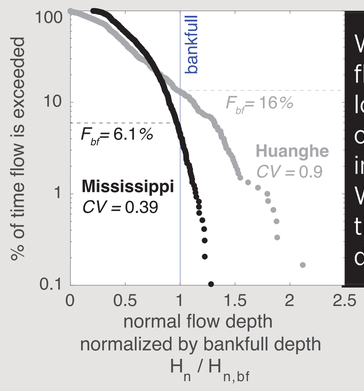

We approximate natural flow variability using a log-normal distribution of stage height upstream in the normal flow reach. We sample the distribution at a user-input flood duration. *(Stedinger et al., 1993)*

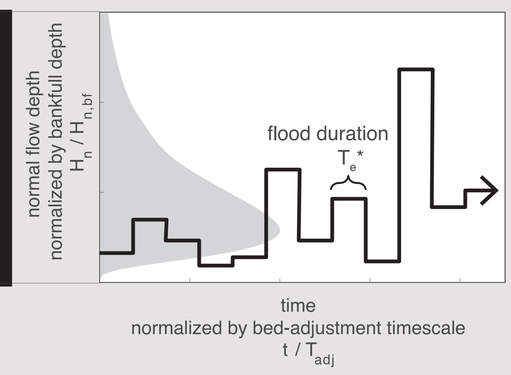

3. Numerical experiments

Constant discharge

After the initial wind-up phase of the simulations, channels avulse throughout the long profile without a preferential avulsion length. Avulsion lengths generally increase through time, and are smaller during episodes of trunk channel sedimentation.

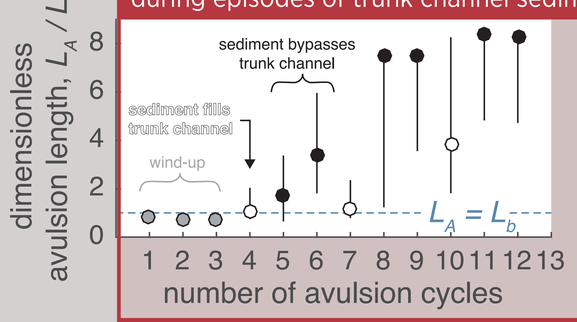

parameter	value
coefficient of variation of normal-flow depth, *CV*	0
bankfull exceedence probability, F_{bf}	N/A
flood duration normalized by adjustment time, T_e^*	N/A

wind-up
sediment fills trunk channel
sediment bypasses trunk channel

Successive lobe profiles feature a self-similar upward concavity, leading to nearly uniform profiles of superelevation upstream of the initial shoreline and a sharp decrease downstream.

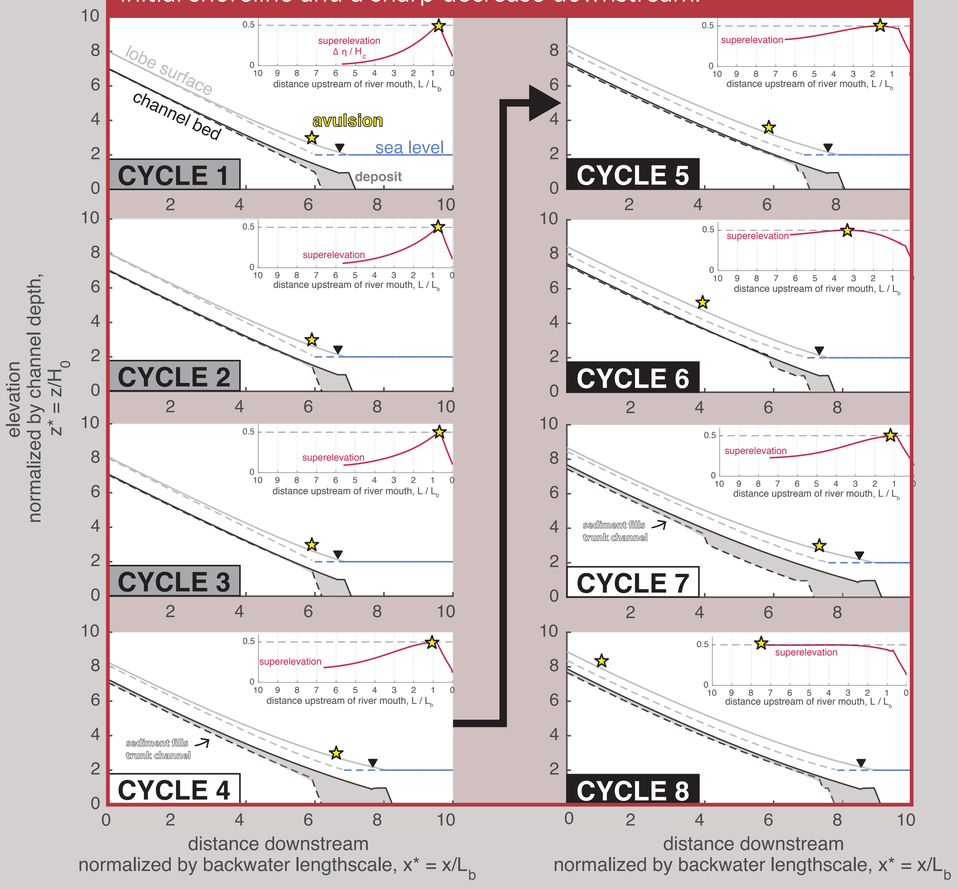

Variable discharge

Variable flood regimes lead to a preferential avulsion length approximately equal to the backwater length. Flow-path selection occasionally creates an erosional wave that triggers an avulsion farther upstream.

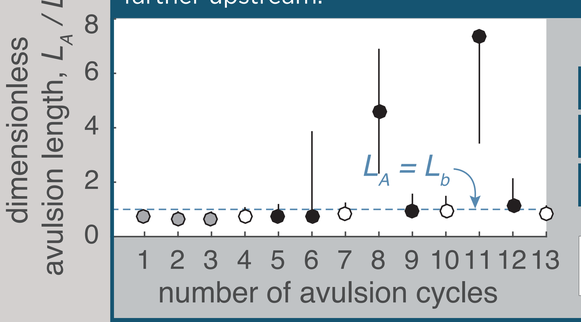

parameter	value
coefficient of variation of normal-flow depth, *CV*	0.5
bankfull exceedence probability, F_{bf}	5%
flood duration normalized by adjustment time, T_e^*	10^{-3}

wind-up
sediment fills trunk channel
sediment bypasses trunk channel

Upward-convexity of the profile in the backwater drives greater superelevation compared to upstream. Downstream, superelevation is reduced because sea level sets the potential energy minimum.

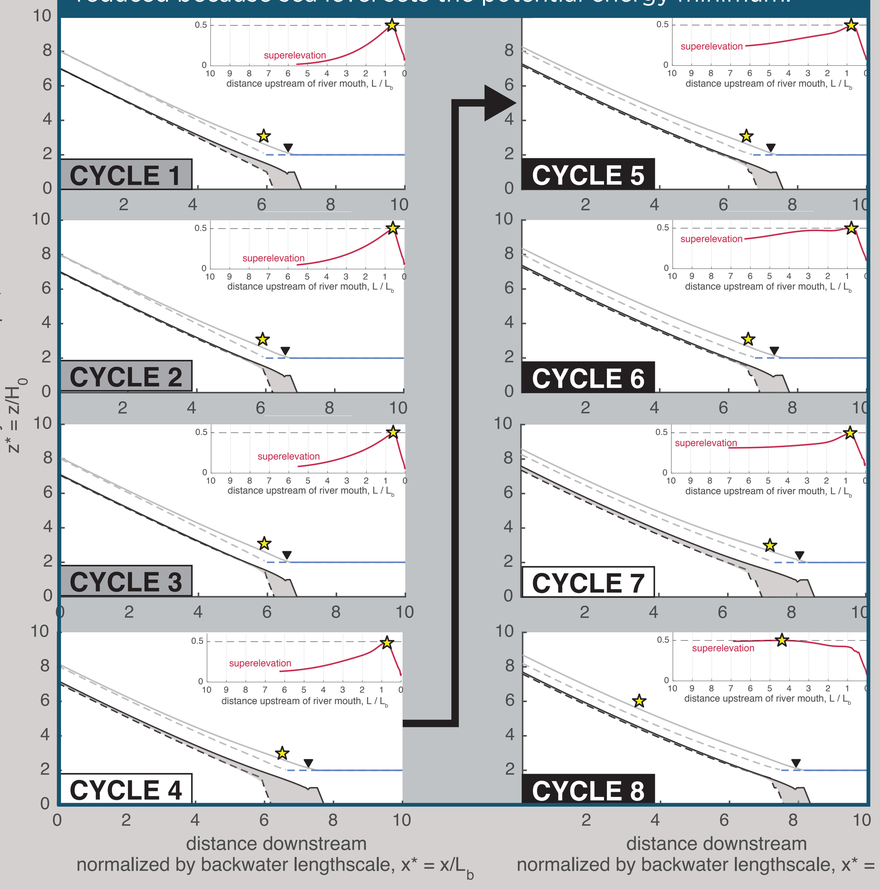

Channels avulse farther upstream when high-flow events are more extreme and more frequent.

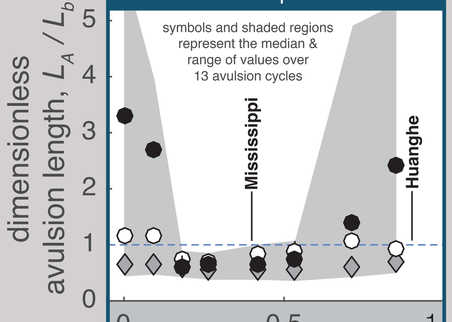

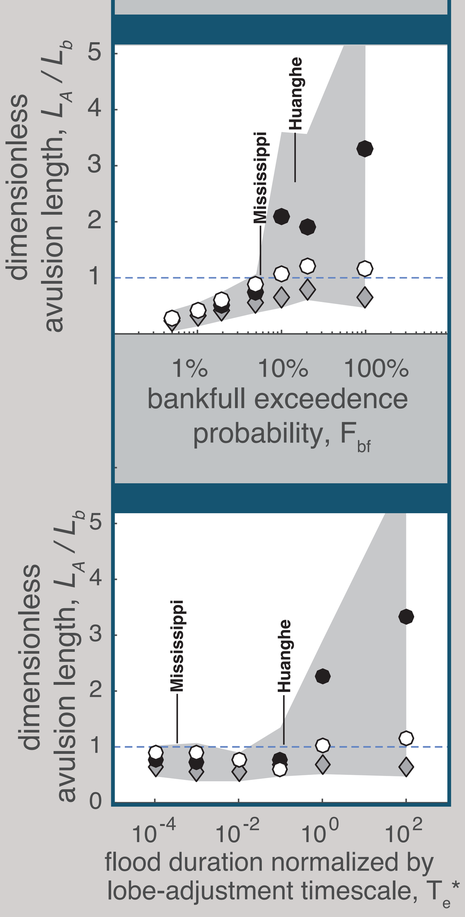

4. Conclusions

We present a predictive model of delta-lobe construction & repeated avulsion that is applicable to deltas over a range of spatial scales, sediment supplies and flood regimes. Delta lobes build on top of one another, demonstrating a distribution of avulsion lengths that is sensitive to flood regime.

Variable flood regimes lead to a preferential avulsion length approximately equal to the backwater length, because intermittent deposition & scour in the backwater zone drives profile upward-convexity and a spatial maximum in superelevation.

Channels avulse farther upstream when high-flow events are more extreme and more frequent.

Chatanantavet, P., Lamb, M. P., & Nittrouer, J. A. (2012). Backwater controls of avulsion location on deltas. Geophysical Research Letters, 39(1).
Chow, V. (1959). Open channel hydraulics. McGraw-Hill Book Company, Inc; New York.
Engelund, F., & Hansen, E. (1967). A monograph on sediment transport in alluvial streams. Technical University of Denmark Ostervoldgade 10, Copenhagen K.
Ganti, V., Chu, Z., Lamb, M. P., Nittrouer, J. A., & Parker, G. (2014). Testing morphodynamic controls on the location and frequency of river avulsions on fans versus deltas: Huanghe (Yellow River), China. Geophysical Research Letters, 41(22), 7882-7890.
Jerolmack, D. J., & Swenson, J. B. (2007). Scaling relationships and evolution of distributary networks on wave-influenced deltas. Geophysical Research Letters, 34(23).
Lamb, M. P., Nittrouer, J. A., Mohrig, D., & Shaw, J. (2012). Backwater and river plume controls on scour upstream of river mouths: Implications for fluvio-deltaic morphodynamics. Journal of Geophysical Research: Earth Surface, 117(F1).
Mohrig, D., Heller, P. L., Paola, C., & Lyons, W. J. (2000). Interpreting avulsion process from ancient alluvial sequences: Guadalope-Matarranya system (northern Spain) and Wasatch Formation (western Colorado). Geological Society of America Bulletin, 112(12), 1787-1803.
Nittrouer, J. A., Shaw, J., Lamb, M. P., & Mohrig, D. (2012). Spatial and temporal trends for water-flow velocity and bed-material sediment transport in the lower Mississippi River. Bulletin, 124(3-4), 400-414.
Paola, C., & Mohrig, D. (1996). Palaeohydraulics revisited: palaeoslope estimation in coarse-grained braided rivers. Basin Research, 8(3), 243-254.
Parker, G. (2004). 1D sediment transport morphodynamics with applications to rivers and turbidity currents. E-book available from http://vtchl. uiuc. edu/people/parkerg/morphodynamics_e-book. htm (last accessed 23 February 2010).
Parker, G., Muto, T., Akamatsu, Y., Dietrich, W. E., & Wesley Lauer, J. (2008). Unravelling the conundrum of river response to rising sea-level from laboratory to field. Part II. The Fly–Strickland River system, Papua New Guinea. Sedimentology, 55(6), 1657-1686.
Stedinger, J. R., Vogel, R. M., & Foufoula-Georgiou, E. (1993). Frequency analysis of extreme events, Chapter 18 in Handbook of Hydrology, edited by DR Maidment.